Loop formation in graphitic nanoribbon edges using furnace heating or Joule heating

JVSTB Journal of Vacuum Science & Technology B

Loop formation in graphitic nanoribbon edges using furnace heating or Joule heating

Xiaoting Jia, Jessica Campos-Delgado, Edgar Eduardo Gracia-Espino, Mario Hofmann, Hiroyuki Muramatsu, Yoong Ahm Kim, Takuya Hayashi, Morinobu Endo, Jing Kong, Mauricio Terrones, and Mildred S. Dresselhaus

Citation: Journal of Vacuum Science & Technology B **27**, 1996 (2009); doi: 10.1116/1.3148829
View online: http://dx.doi.org/10.1116/1.3148829
View Table of Contents: http://scitation.aip.org/content/avs/journal/jvstb/27/4?ver=pdfcov
Published by the AVS: Science & Technology of Materials, Interfaces, and Processing

Loop formation in graphitic nanoribbon edges using furnace heating or Joule heating

Xiaoting Jia[a)]
Department of Materials Science and Engineering, Massachusetts Institute of Technology, Cambridge, Massachusetts 02139-4307

Jessica Campos-Delgado[a)] and Edgar Eduardo Gracia-Espino
Department of Advanced Materials and Laboratory for Nanoscience and Nanotechnology Research (LINAN), IPICYT, Camino a la Presa San José 2055, Col. Lomas 4a. sección, San Luis Potosí 78216, México

Mario Hofmann
Department of Electrical Engineering and Computer Science, Massachusetts Institute of Technology, Cambridge, Massachusetts 02139-4307

Hiroyuki Muramatsu, Yoong Ahm Kim, Takuya Hayashi, and Morinobu Endo
Faculty of Engineering, Shinshu University, 4-17-1 Wakasato, Nagano 380-8553, Japan

Jing Kong
Department of Electrical Engineering and Computer Science, Massachusetts Institute of Technology, Cambridge, Massachusetts 02139-4307

Mauricio Terrones
Department of Advanced Materials and Laboratory for Nanoscience and Nanotechnology Research (LINAN), IPICYT, Camino a la Presa San José 2055, Col. Lomas 4a. sección, San Luis Potosí 78216, México

Mildred S. Dresselhaus[b)]
Department of Electrical Engineering and Computer Science, Massachusetts Institute of Technology, Cambridge, Massachusetts 02139-4307 and Department of Physics, Massachusetts Institute of Technology, Cambridge, Massachusetts 02139-4307

(Received 26 February 2009; accepted 11 May 2009; published 30 July 2009)

Here the authors report the use of either furnace heating or Joule heating to pacify the exposed graphene edges by loop formation in a novel graphitic nanoribbon material, grown by chemical vapor deposition. The edge energy minimization process involves the formation of loops between adjacent graphene layers within the nanoribbons. A comparison is made of the similarities and differences between the loop structures formed using these two methods. An estimation of the temperature of these graphitic nanoribbons during Joule heating is also reported based on the melting and evaporation of Pt nanoparticles. © *2009 American Vacuum Society.*
[DOI: 10.1116/1.3148829]

I. INTRODUCTION

Recently, carbon nanomaterials such as carbon nanotubes,[1] graphene,[2] and graphitic nanoribbons[3] have attracted much attention because of their unique and fascinating physical properties. It has also been reported that when graphitic materials are subjected to high temperatures (e.g., $>1500\ ^\circ C$), the ends of the graphitic sheets find a more stable configuration by forming a loop with an adjacent sheet,[4–10] thereby healing the dangling bonds at the edge sites. These loops exhibit a diameter larger than the sheet-to-sheet separation of the graphene layers. Double and multiple layered loops have also been observed in these experiments. The loop formation phenomenon is surface driven and strongly involves the physics and chemistry of reactive edges and sp^2 hybridized surfaces and interfaces. This report focuses on the loop formation in graphitic nanoribbons based on furnace heating and Joule heating, and reports similarities and differences between the loops formed by the two complementary methods.

To the best of our knowledge, the first experimental observation of loop formation at the edges of graphitic layers was reported by Murayama *et al.*[4] in 1990 in furnace heat treated graphite filaments. Since then, experimental evidence of loop formation has been provided in various furnace heat treated graphitic materials,[5–10] such as graphite polyhedral crystals[5] and cup-stacked nanofibers.[6] The transitional evolution of such loops from active end planes to stable loop configurations caused by annealing was first reported by Endo *et al.*[7] Liu *et al.*[10] also reported that loops are formed from graphite edges after furnace heat treatment at 2000 °C for 3 h. Most recently, Campos-Delgado *et al.*[9] reported defect annealing and loop formation in graphene nanoribbons for heat treatment temperatures up to 2800 °C and they also reported their transformational mechanism and properties.

Joule heating has also provided an efficient way to achieve high temperatures in many carbon materials, and it has been demonstrated that carbon nanostructures could be

[a)]Authors contributed equally to this publication.
[b)]Author to whom correspondence should be addressed; electronic mail: millie@mgm.mit.edu

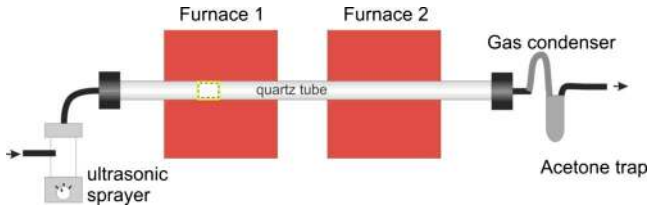

FIG. 1. (Color online) Schematic of the experimental setup used in the synthesis of graphitic nanoribbons. The marked area in the tube within furnace 1 corresponds to the region where the graphitic nanoribbon material is deposited during synthesis.

modified substantially by Joule heating, showing phenomena, such as the superplasticity of carbon nanotubes,[12] wall-by-wall breakdown of multiwall carbon nanotubes,[13] and the formation of tubular structures from amorphous carbon nanowires by Joule heating.[14] In particular, graphitic nanoribbons[3] represent an outstanding system to study edges and loop formation because of the high density of accessible end planes that are present in this material. Characteristic changes in the structure of graphitic nanoribbons have already been reported[9] when high temperatures come into play. In the present work we describe two routes to create loops on the edges of graphitic nanoribbons: One is through conventional furnace heating, and the other is through Joule heating. A detailed description of the synthesis process of this interesting material is included at the beginning of this article, as well as a brief discussion of the morphology and structure of this material, obtained by electron microscopy. In this work, we also compare the results of loop formation for the two cases of Joule heating and furnace heating, showing both similarities and complementary behaviors.

II. EXPERIMENTS AND DISCUSSION

In this long section we review the synthesis of the novel graphitic nanoribbon material (Sec. II A) followed by a discussion of loop formation in this novel material by furnace annealing (Sec. II B), and by Joule heating (Sec. II C). Estimates of temperatures that can be achieved in samples of graphitic nanoribbons within the transmission electron microscope (TEM) are obtained from phase transition measurements carried out on Pt nanoparticles (Sec. II D) and this discussion is followed by a summary discussion on possible mechanisms for loop formation in these nanoribbons (Sec. II E).

A. Novel graphitic material

1. Synthesis details

The experimental setup used in the synthesis of graphitic nanoribbons[3] is shown schematically in Fig. 1, where all the necessary equipment is placed inside a fume hood. A quartz tube (~1.1 m long), connecting an ultrasonic sprayer and a gas condenser/acetone trap for the exiting gases, is placed inside two tubular furnaces (see Fig. 1). The length of each furnace is 40 cm and the separation between the two furnaces is ~15 cm. An inert atmosphere is maintained by flowing argon gas through the system. A solution containing 280 ml of ethanol, 2.8235 mg of ferrocene ($FeC_{10}H_{10}$), and 0.266 ml of thiophene (C_4H_4S) is prepared and placed inside the ultrasonic sprayer. During the heating of the furnaces, the ultrasonic sprayer is kept turned off and the flow of Ar is set to 0.2 l/min. Once both furnaces reach 950 °C, the ultrasonic sprayer is turned on. The aerosol produced is carried to the hot zone of the furnaces by raising the flow rate to 0.8 l/min. These conditions are maintained for 30 min, after which the sprayer is turned off, the flow rate is decreased to 0.2 l/min, and the two furnaces are allowed to cool down to room temperature.

Once the system has cooled down, the quartz tube is taken out and the material of interest containing the nanoribbons is scraped from the walls of the tube. The nanoribbons are deposited as a powder within furnace 1 in a region between 12 and 20 cm relative to the left edge position of the first furnace (see Fig. 1).

The black powder containing the nanoribbons has been shown to be efficiently dispersible in various alcohols. We have used ethanol and methanol followed by sonication to create suspensions of graphitic nanoribbons. These suspensions have been used to prepare samples mounted on copper grid sample holders for use in scanning electron microscope (SEM) and TEM observations.

The morphology of the nanoribbons as observed by SEM and TEM is depicted in Fig. 2. A low magnification image of the as-produced nanoribbons is shown in Fig. 2(a). The di-

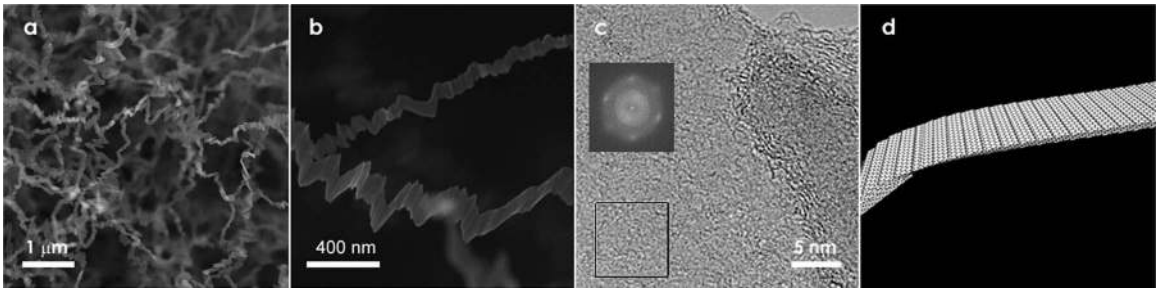

FIG. 2. SEM and TEM images of as-produced graphitic nanoribbons. (a) Low magnification SEM image, where a very clean material with no by-products is seen. (b) Higher magnification SEM image of the same sample as in (a). (c) TEM image of the surface of the nanoribbon, where the ribbon edge and the structure of a ripple are shown in the right-hand side of the image. The inset represents the FFT of the square region showing the sixfold symmetry of the diffraction pattern. (d) A simulated morphology of the ribbon samples showing the ripples as consisting of individual graphitic sheets with open edges.

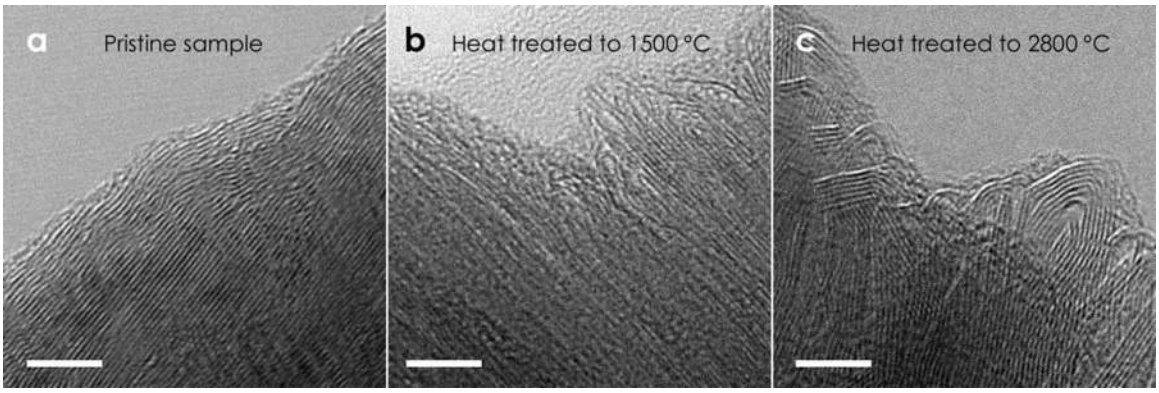

FIG. 3. TEM micrographs of the edges of graphitic nanoribbons: (a) pristine sample, (b) sample heat treated at 1500 °C, and (c) sample heat treated at 2800 °C for 30 min in graphite furnace under an inert Ar atmosphere (Ref. 9). The scale bars for the three images correspond to 5 nm.

mensions of the nanoribbons range from 80 to 500 nm in width, up to 10–15 nm in thickness, and many microns in length. The material shows ripples along the main axis, as observed in Fig. 2(b). Because of these ripples, the ribbons have a discontinuous appearance. It is also noteworthy that in our TEM observations, we could not find catalytic Fe particles attached to the material or embedded in the entangled nanoribbons.

TEM characterization of the graphitic nanoribbon material[3] reveals a crystalline structure with 001 planes parallel to the ribbon main axis. The fast Fourier transform (FFT) in the inset of Fig. 2(c) shows that the graphitic nanoribbons are crystalline, consistent with a honeycomb lattice structure. The nanoribbon structure is sketched in Fig. 2(d) to help clarify the essence of their structural morphology.

Elemental analysis by x-ray photoelectron spectroscopy (XPS) showed that the nanoribbons consist of C and some oxygenated groups,[3] which we believe are attached to the edges of the ribbons, and these chemical groups thereby passivate these edges. Other atoms present in the synthesis, such as S or Fe, were not detected in our measurements due to their lower concentration when compared to the detection limits of the different techniques used (energy dispersive x-ray analysis, electron energy loss spectroscopy, XPS). Nevertheless, it is possible that some low concentrations of heteroatoms are incorporated into the sp^2 hybridized lattice, along with O and H.

B. Loop formation by furnace heating

The as-produced nanoribbon material was annealed at various temperatures between 1500 and 2800 °C using a graphite furnace under an inert Ar atmosphere for 30 min.[9] The structural changes promoted by furnace heating of the samples were monitored by TEM, as shown in Fig. 3 by comparing the images for the pristine material [Fig. 3(a)] and for the samples annealed at 1500 °C [Fig. 3(b)] and at 2800 °C [Fig. 3(c)] within the graphite furnace.

For the pristine (as-prepared) sample,[3] we can observe relatively straight lattice fringes and open end planes at the edges of the unannealed nanoribbon. After a heat treatment at 1500 °C, we can notice some changes in the structure, including a straightening of the lattice fringes, reflecting a restructuring process, which also includes single loop formation at the edges. In contrast, for the pristine sample only open-ended planes were observed. At the highest heat treatment temperature (2800 °C), we observe in Fig. 3(c) multiple loops with highly faceted morphologies, along with a highly crystallized material away from the edges of the sample.

Further characterization of the heat treated (HT) graphitic nanoribbons[9] is shown in Fig. 4. Thermogravimetric analysis (TGA) [Fig. 4(a)] revealed the decomposition temperatures T_d in air of the three investigated samples (pristine, HT at 1500 °C and HT at 2800 °C), with values of T_d being 702, 772, and 780 °C, respectively. We can conclude that the annealing treatment induces structural changes that turn the sample into a less reactive material since the decomposition temperature for the pristine material was increased by ~70 °C through heat treatment at 1500 °C. Only an increase of 8 °C in T_d was found by further increase of the heat treatment process to 2800 °C. These changes in the structure were also confirmed by Raman spectroscopy [see Fig. 4(b)]. For the pristine sample we note a very high intensity of the *D* band, even higher than for the *G* band, indicating that the hexagonal symmetry of the carbon lattice is bro-

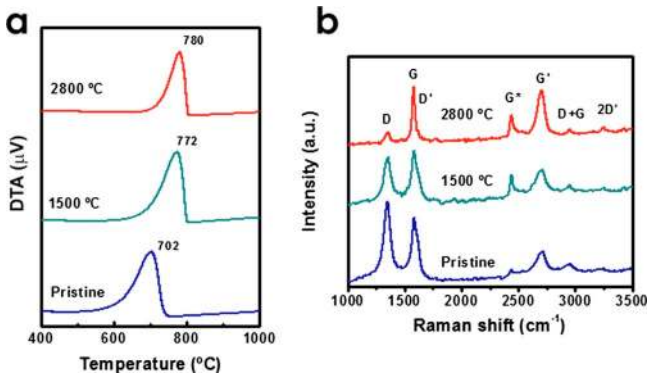

FIG. 4. (Color online) (a) Data on graphitic ribbons for the first derivative with respect to temperature of the weight loss curves (Ref. 9) and (b) Raman spectra at E_{laser}=2.33 eV for the pristine sample and the samples heat treated at 1500 and 2800 °C (adapted from Ref. 9).

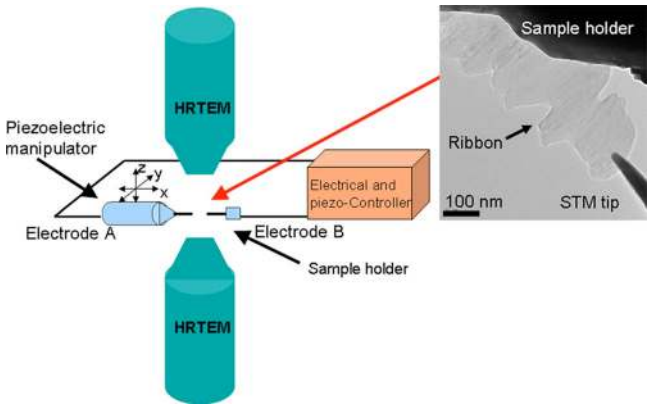

FIG. 5. (Color online) Schematic of the TEM-STM system. The inset on the right shows a low magnification TEM image of a nanoribbon piece placed in between two electrodes (the sample holder and the STM tip).

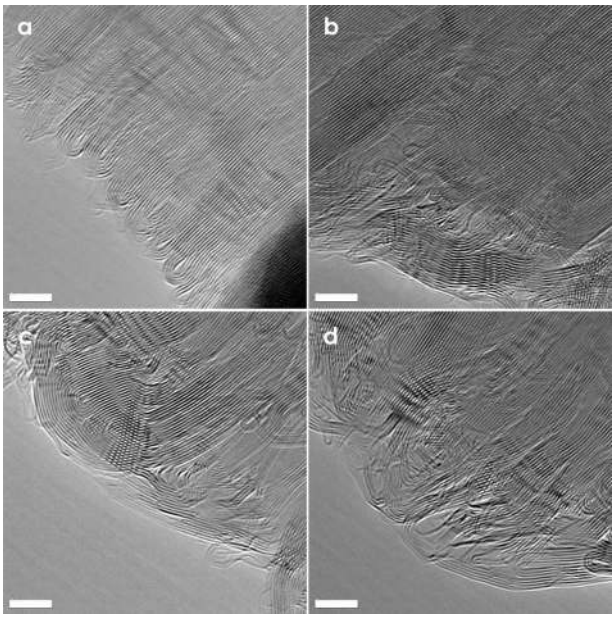

FIG. 6. TEM images showing loop formation by Joule heating: (a) near the electrode, [(b) and (c)] further away from the electrodes than in (a), and (d) near the central region of the suspended graphitic nanoribbon material (scale bar is 5 nm).

ken due to the presence of structural defects; as the annealing temperature is increased to 1500 °C, we notice a considerable decrease in the *D*-band intensity. This is in good agreement with both the TEM and the TGA results, indicating a transformation into a more crystalline material with annealing at 1500 °C. The similarity of T_d for both the HT-1500 °C and HT-2800 °C samples suggests that little change in chemical reactivity occurs with further heat treatment above 1500 °C. The HT-2800 °C sample, however, showed a residual Raman *D* band with a low intensity because energetically stable loops formed in the end planes of nanoribbons prevent the development of three-dimensional stacking, which we attribute to a high degree of graphitization in the material as a whole. However, the loops formed by heat treatment and the ripples that were preserved within the ribbons after heat treatment are both types of symmetry-breaking structures that induce a residual *D*-band intensity. Heat treatment also enhances the intensities of the G^*-band ($\sim$2450 cm^{-1}) and the G'-band ($\sim$2700 cm^{-1}) features in Fig. 4 which are second order combination modes and harmonics of the *D*-band feature, respectively.[11] The intensities of these modes are typically enhanced by increased structural order, in contrast to the *D*-band intensity which is suppressed by structural order.

C. Loop formation by Joule heating of the graphitic ribbon material

Resistive Joule heating experiments on the graphitic nanoribbons were carried out using an integrated scanning tunnel microscope (STM)-TEM system (a JEOL 2010F high resolution TEM integrated with a Nanofactory STM holder) which is further attached to a piezoelectric stage that allows us to move the tip in all 3 (x,y,z) directions (see Fig. 5). The STM tip and sample holder also serve as two electrodes. The as-prepared ribbon sample is placed in between the STM tip and the sample holder, and a controlled bias voltage is applied across the ribbon.

Figures 6(a)–6(d) depict TEM images of the nanoribbon edges after Joule heating. As we can see from these images, in the interior region of the ribbon material, the originally wavy fringes [see Figs. 2(c) and 3(a)] are developed into close packed straight lines, indicating an increased crystallinity of the graphitic nanoribbon material, which is consistent with our observation of furnace-heated samples at 1500 and 2800 °C [Figs. 3(b) and 3(c)].[9] Along the edges of the ribbon material, the open ends [Fig. 3(a)] disappear, thus forming loops of different shapes [Figs. 6(a)–6(d)]. The loops formed near the electrodes [Fig. 6(a)] reveal a larger degree of curvature with a minimum of two to three layers contained within the loops, a result which is consistent with the furnace-heated samples in the temperature range between 2000 and 2500 °C.[9] The loops formed further away from the electrodes [Figs. 6(b) and 6(c)] display a smaller curvature with more than ten layers contained on average within a single loop. Finally, the loops formed near the central region of the ribbon material [Fig. 6(d)] reveal even larger loops and these even contain some facets (graphitization effect). Compared to the furnace heat treatment at 2800 °C [Fig. 3(c)] where multiple loops (approximately six layers) are formed, Joule heating [Figs. 6(c) and 6(d)] results in loop formation with more layers (greater than ten layers), which might indicate that a higher local temperature is reached. Furthermore, the annealing process for Joule heating takes a shorter time ($\sim$15 min) compared to 30 min in the furnace heating experiment.[9]

The effect of loop formation by Joule heating is primarily attributed to the high temperature achieved by resistive Joule heating. We attribute the different shapes of the loops, that are smaller loops (double or triple) near the electrodes [Fig. 6(a)], and larger multiple loops and faceted formations near the central region of the ribbon [Fig. 6(d)], to the larger

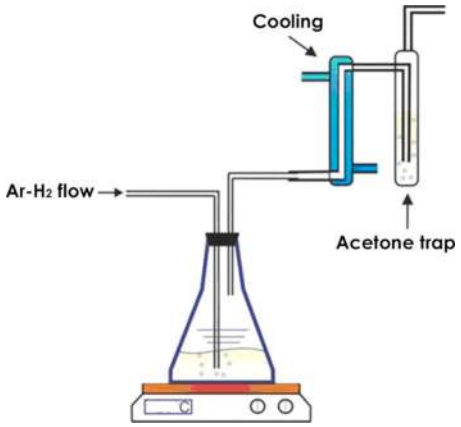

FIG. 7. (Color online) Diagram of the setup used in the process of anchoring Pt nanoparticles to the graphitic nanoribbon material.

temperature difference across the ribbon. Here the two electrodes serve as the heat sinks, and good thermal conductivity is achieved near the electrodes so the temperature near the electrodes is much lower than that in the central region of the ribbon. This result is also consistent with the furnace heating experiments, which showed that different shapes of loops are formed at different annealing temperatures [Figs. 3(a)–3(c)]. The loop formation in graphitic nanoribbon edges by Joule heating does not contradict the sharp edge reconstruction observed during Joule Heating.[15] In the latter, it was demonstrated that electron beam irradiation of ribbon samples, prior to Joule heating (between 10–15 min), plays a key role in the edge reconstruction process. This irradiation damages considerably the structure, leading to the creation of vacancies, interstitials and, most importantly, the sheets edges become irregular and unparallel, probably due to the indistinctive evaporation of C species. This damage is evident in the image of the nanoribbon before Joule heating in the supporting online material of Ref. 16. Therefore, this irregularity of the edges does not favor the loop formation between adjacent layers, but the sharp edge reconstruction during the Joule heating process.[16]

When an as-produced nanoribbon is subjected to Joule heating without electron beam irradiation, as discussed in this work, there is a significant rise in temperature. This increase in temperature results in the annealing of defects, in-plane crystallinization, and the adjacent sheets find a more stable configuration by forming loops, as observed in the furnace heating treatments,[9] and Iijima's recent work.[10]

D. Temperature estimates for the Joule heating experiment

In order to estimate the temperature of the graphitic nanoribbons during the Joule heating experiment, Pt nanoparticles were deposited chemically on the as-prepared nanoribbon surface [Fig. 7(a)], and the structural changes in the Pt nanoparticles were monitored *in situ*. The Pt decoration process consisted of sonicating for 15 min a mixture of graphitic nanoribbons (10 mg), plus 10 ml of *N*,*N*-dimethylformamide (Sigma-Aldrich®, 99%), (1,5-Cyclooctadiene) dimethylplatinum(II) (Sigma-Aldrich®, 97%) as a platinum source and polyvinylpyrrolidone (Sigma-Aldrich®, average molecular weight of 10 000) as a passivating agent. After sonication, the suspension was maintained under an $Ar-H_2$ (5% H_2) atmosphere to increase the reduction rate (see Fig. 7), and the suspension was subsequently placed in a glycerin bath at 110 °C for 40 min.

Next, the suspension was allowed to cool down to room temperature and the composite material (graphitic nanoribbons with Pt particles) was recovered by filtration. These graphitic nanoribbons exhibited Pt nanoparticles (with an average size of ~6 nm) anchored to their surface. Finally a thermal treatment was carried out at 350 °C under an Ar atmosphere for 15 min in order to remove any residues of organic material that could remain on the surface of the composite material.

The modified nanoribbon material was then mounted on the TEM-Joule heating setup. As we increased the applied voltage across the nanoribbons, the Pt nanoparticles near the central region of the ribbon started to melt and merge with small neighboring Pt nanoparticles (some particles finally reached a diameter of 13 nm). Subsequently, and starting from the central region, the Pt nanoparticles evaporated, resulting in a clean surface (devoid of Pt nanoparticles) near the center of the ribbon sample [Fig. 8(b)]. When a higher voltage is applied, additional Pt nanoparticles evaporate and eventually almost the entire ribbon is free of Pt nanoparticles [Fig. 8(c)]. From these experiments, we confirmed that good thermal contacts are made near the electrodes, and that the two electrodes serve as heat sinks. The central region of the ribbon [Fig. 8(c)] exhibits the highest temperature at a given applied voltage.

Given the bulk Pt boiling point of 3827 °C, and that the boiling point of the Pt nanoparticles will have a lower boiling point than their bulk counterpart material due to size effects,[15] we estimate the temperature of the suspended ribbon sample under Joule heating to be above 2800 °C based on the loop formation morphology [comparison of Figs. 3(c) and 6(d)].

E. Proposed mechanism for loop formation

We have demonstrated that loop formation through the coalescence of bare edges on nearby graphene sheets can be successfully achieved by both furnace annealing and Joule heating. We have also noted that high temperatures play the main role in this process. As explained by Campos-Delgado *et al.*,[9] the loop formation is the result of a restructuring process taking place in the nanoribbons when subjected to high temperatures. As the annealing temperature is increased to 1500 °C, the experiments carried out with the furnace reveal that the structure becomes much more crystalline; the lattice fringes seen in the TEM images corresponding to graphitic planes straighten up as the annealing temperature is increased. Above this temperature, the edges of the ribbons reconstruct, and single loops start appearing. It is noteworthy

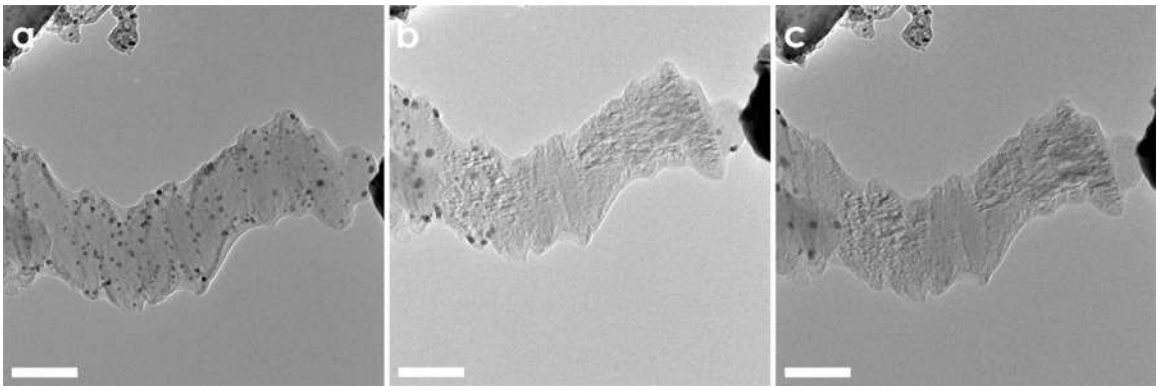

FIG. 8. Sequence of TEM images showing Pt nanoparticles on the ribbon surface (a) before Joule heating, (b) after Joule heating for 11 min under a constant bias of ~2 V, and (c) after Joule heating for another 4 min under a constant bias of ~2 V. Here we see that the Pt particles melt and merge into bigger clusters (b), and start to evaporate from the central region of the ribbon (b), and eventually evaporate across almost the entire ribbon sample (c) (scale bar is 100 nm).

that the diameter of these loops is larger than the sheet-to-sheet separation, sketched in Fig. 9 and observed experimentally in Fig. 3(b).

Annealing temperatures around 2000 °C result in double loop formation (see Fig. 9), as reported previously in Refs. 9 and 10. At higher temperatures, above 2500 °C, multiple loops form and we also observed more faceted graphitic features.

For the Joule heated nanoribbons, a similar high temperature effect is achieved due to resistive Joule heating. However, a higher degree of crystallinity is achieved with increased annealing by Joule heating, and loops are created in the graphitic nanoribbon material in order to passivate the carbon atoms at the edges. However, when compared to the furnace heat treatment results, Joule heating could reach higher local temperatures ($\gg$2500 °C) in the material, which induce enhanced crystallinity by the formation of larger multilayered loop structures. It is also important to emphasize that the loop formation and the lattice restructuring process could be achieved in a relatively short annealing time by Joule heating.

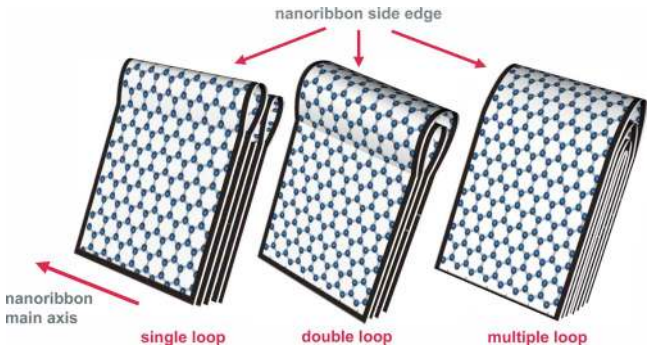

FIG. 9. (Color online) Schematic model of single, double, and multiple loops formed in the graphitic nanoribbons, where the direction along the length of the nanoribbon is considered as the main axis [see also Figs. 2(b) and 2(d)].

III. CONCLUSIONS AND OUTLOOK

In this work we discussed the structural transformations occurring in a novel type of high surface area graphitic nanoribbon material grown by a chemical vapor deposition method, which is especially well suited for studying edge reconstruction[3] and for studying loop formation. In this article we investigated loop formation in these graphitic nanoribbons, under both furnace heating and Joule heating; these provide complementary ways of heating the samples. In both cases, the pristine open edges of the nanoribbons are shown to develop into stable closed loops, and the shapes and sizes of the loops could be modified and controlled by varying the annealing temperature and other annealing conditions. The Pt nanoparticle evaporation experiment confirms that high temperatures can be achieved with the Joule heating of suspended graphitic nanoribbons, and the shapes of the loops under Joule heating provide evidence for edge evolution into multiloop structures above 2500 °C. Comparing furnace heating and Joule heating we can conclude that Joule heating could be an efficient way for restructuring pregraphitic structures into highly ordered graphitic material, in which stable loops could be formed after an edge reconstruction process of the bare edges of the laminated carbon material has taken place. We envisage that the chemistry and reactivity of these loops will be different when compared to the precursor materials. Therefore, the interaction of different molecules with these loop structures should now be studied from the experimental and theoretical standpoint, so that these looped edges could be used as sensors.

ACKNOWLEDGMENTS

The authors thank Gene Dresselhaus for valuable and fruitful discussions. This work was supported by the NSF under Grant Nos. NIRT CTS-05-06830 and DMR 07-04197, and MIT-CONACYT collaboration grant. The Mexican authors also acknowledge CONACYT-Mexico for Grant Nos. 56787 (Laboratory for Nanoscience and Nanotechnology

Research-LINAN), 45772 (M.T.), 58899 (Inter American Collaboration) (M.T.), and 2004-01-013/SALUD-CONACYT (M.T.), and Ph.D. scholarships (JCD, EEGE).

[1]S. Iijima and T. Ichihashi, Nature (London) **363**, 603 (1993).
[2]K. S. Novoselov, A. K. Geim, S. V. Morozov, D. Jiang, Y. Zhang, S. V. Dubonos, I. V. Grigorieva, and A. A. Firsov, Science **306**, 666 (2004).
[3]J. Campos-Delgado *et al.*, Nano Lett. **8**, 2773 (2008).
[4]H. Murayama and T. Maeda, Nature (London) **345**, 791 (1990).
[5]Y. Gogotsi, J. A. Libera, N. Kalashnikov, and M. Yoshimura, Science **290**, 317 (2000).
[6]M. Endo *et al.*, Appl. Phys. Lett. **80**, 1267 (2002).
[7]M. Endo *et al.*, New J. Phys. **5**, 121.1 (2003).
[8]M. José-Yacamán, H. Terrones, L. Rendón, and J. M. Domínguez, Carbon **33**, 669 (1995).
[9]J. Campos-Delgado *et al.*, Chem. Phys. Lett. **469**, 177 (2009).
[10]Z. Liu, K. Suenaga, P. J. F. Harris, and S. Iijima, Phys. Rev. Lett. **102**, 015501 (2009).
[11]M. S. Dresselhaus, G. Dresselhaus, R. Saito, and A. Jorio, Phys. Rep. **409**, 47 (2005).
[12]J. Y. Huang *et al.*, Nature (London) **439**, 281 (2006).
[13]J. Y. Huang, S. Chen, S. H. Jo, Z. Wang, D. X. Han, G. Chen, M. S. Dresselhaus, and Z. F. Ren, Phys. Rev. Lett. **94**, 236802 (2005).
[14]J. Y. Huang, S. Chen, Z. F. Ren, G. Chen, and M. S. Dresselhaus, Nano Lett. **6**, 1699 (2006).
[15]M. Attarian Shandiz, J. Phys.: Condens. Matter **20**, 325237 (2008).
[16]X. Jia *et al.*, Science **323**, 1701 (2009).